Computational Fluid Dynamics Study of Wind Turbine Blade at Low Reynolds Number for Various Angle of At-tack

Ayushman Mishra

[1]*Alumnus, Delhi Technological University, Delhi, India*

ABSTRACT: Nowadays, renewable energy is the primary source of clean en- ergy. Wind energy, among other renewable energy sources, has emerged as one of the most important solutions to the current energy crisis. The aerodynamic performance of the wind turbine blade must be evaluated in order to produce the most power in an economic way through using a wind turbine. The lift and drag coefficients are important parameters to consider when analysing wind turbine blade performance. The maximum sliding ratio is desired in order to obtain the most power from the wind turbine. This paper aims to deal with the numerical investigation of wind turbine blade (S821 airfoil) aerodynamic characteristics at the chord Reynolds number of Re $= 0.68 \times 10^5$. The numerical simulations of the flow around wind turbine blade have been carried out by using the com- putational fluid dynamics (CFD) software; ANSYS workbench. A nu- merical investigation of the low speed flows around the wind turbine blade is presented using k- ε turbulent model. The recorded maximum coefficient of lift and sliding ratio are observed to be 0.8447 at 22° angle of attack and 4.42 at 8° angle of attack. The comparison with literature results shows that the CFD approach used in this study can accurately predict the aerodynamic characteristics of wind turbine blade. We be- lieve that the results shown in this paper will be useful for wind turbine blade design engineers.

Keywords: Wind turbine blade, CFD, Sliding ratio, Aerodynamic char-acteristics

I. INTRODUCTION

The global demand for energy is increasing on a daily basis. There is no hope for its reduction because the population and thus demand will continue to grow. It is extremely difficult to meet all of the demand in such an increasing demand, and even if it is met, it will result in environmental pollution and other negative consequences for the envi- ronment, as the majority of today's energy is generated by non-renewable energy sources [1].

Wind power has the most promising prospects of any renewable or sustainable en- ergy technology. Furthermore, wind energy is becoming more popular around the world because it is available everywhere and is a useful renewable energy source that does not contribute to global warming due to radiation [2]. Wind energy construction effi- ciency is becoming increasingly important as the global use of wind energy grows. Furthermore, wind energy is a low-density power source. To make wind power eco- nomically viable, the efficiency of converting wind energy into mechanical energy must be maximised [3].

Horizontal Axis Wind Turbines (HAWT) and Vertical Axis Wind Turbines (VAWT) are the two types of wind turbines. Horizontal turbines have blades that rotate in a plane perpendicular to the axis of rotation. HAWTs are the most common type of wind turbine and come in a variety of sizes and shapes. Drag forces are the most com- mon type of force acting on HAWT blades. The rotation axis coincides with the axis of power generation in Vertical Axis Wind Turbine blades [6]. A wind turbine is made up of several major components, including the rotor, generator, driven chain, control sys-tem, and so on. The wind drives the rotor, which rotates at a predetermined speed about the wind speed, allowing the generator to produce electric energy under the control regulation of the system. To obtain the greatest amount of kinetic energy from wind, many people have put a lot of time and effort into the design of an effective geometry.

Many research papers have been published so far on various wind turbine blade pro-files for the 2D airfoil, and limited papers in the case of the 3D wind turbine blade. Few examples are, Mohamed A et al., (2012), studied aerodynamic analysis of an

S-series wind turbine blade which has been performed using the Computational Fluid Dynamics (CFD) method based on the finite-volume approach. The performance of various blade profiles at various wind speeds has been investigated, and the optimum blade profile for each wind speed has been determined using the maximum sliding ratio. It has been concluded that the CFD code in this study can correctly predict the aerodynamic loads on wind turbines [4]. For the simulation, various wind speeds in Egypt have been used to produce profiles for Egypt's weather conditions. Hoogedoorn et al., has also per- formed 2D CFD-RANS simulations at high Reynolds numbers for the wind turbine blade profiles NACA 0008 and NACA0012 [5]. As a result, the research articles avail- able on HAWT's aerodynamic performance analysis mostly focus on the range of high wind speeds, with very few studies focusing on the low-speed range.

Although the wind turbine blade aerodynamic performance has been a hot topic in the non-renewable energy sources for quite some time, the present study quantifies the wind turbine blade aerodynamic performance characteristics under the influence of low-speed range through using the ANSYS workbench. The wind turbine blade profile selected based on the previous research carried out by M. M. M. Talukder et al., (2016). The objective of the current research is to fill the above-mentioned research gap and outline the possible effectiveness and usability of a wind turbine blade for HAWT ap- plications. The purpose of our research is twofold: Firstly, to investigate the feasibility of a numerical simulation approach with the aim of studying the effect of the aerody- namic loads on the wind turbine blade; Secondly, to analyze the impact of the aerody-namic loads under the influence of low-speed range with the aim of understanding the effectiveness and usability of a wind turbine blade. The numerical data obtained are compared with experimental data [7].

II. NUMERICAL APPROACH

The numerical simulations of the flow around wind turbine blade have been carried out through using the commercial CFD software; ANSYS workbench. A C – type do- main has been created around the solid body, and then the fluid volume has been ex- tracted for analysis, as shown in Figure 1. The total number of elements and nodes found are 1.9 million and 2.01 million. Figure 2 shows the 3D computational grid gen-eration and boundary conditions over the wind turbine blade. The numerical simulation has been performed for a different angle of attack, i.e. -4° to 30° at Reynolds num- ber 0.68×10^5, the flow model is considered as standard k-ε turbulent. Residual target for convergence criteria has been set at $1*E^{-6}$.

The wind turbine blade airfoil (S821) coordinates extracted from NREL's airfoil database [8]. The far-field incoming air has a velocity of 5 m/s [$chord based (c = 0.2\ m) Re = 0.68 \times 10^5$] at a different angle of attack i.e. -4° to 30°.
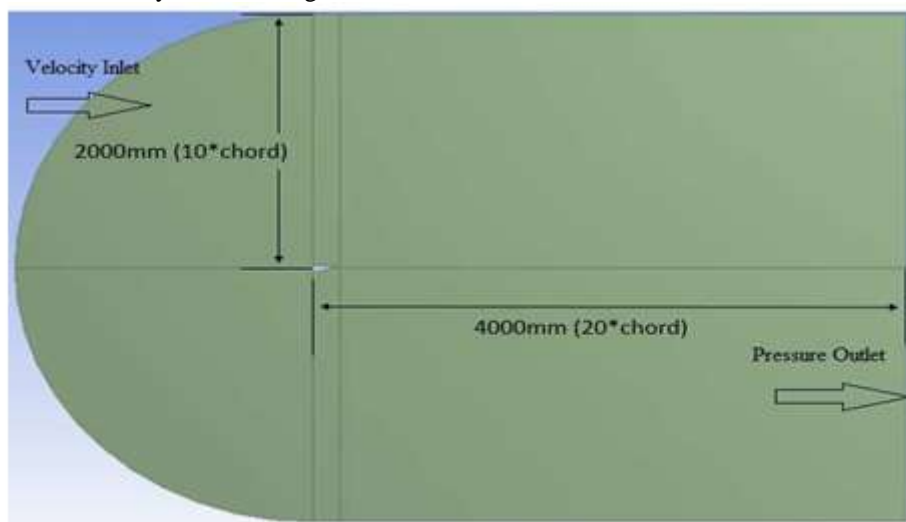

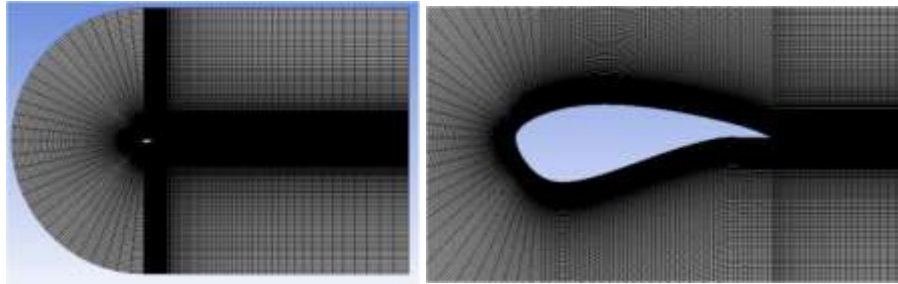**Fig. 1.** C-Type Domain around the wind turbine blade with boundary conditions

Fig. 2. 3D Computational grid around the wind turbine blade

In this study, the aerodynamic characteristics of the wind turbine blade are calculated by the coefficients of lift and drag, which are defined as follows:

$$C_l = \frac{L}{1/2\rho_\infty v_\infty^2 c} \quad Eq.\ 1$$

$$C_d = \frac{D}{1/2\rho_\infty v_\infty^2 c} \quad Eq.\ 2$$

Where C_d is the drag coefficient and C_l is the lift coefficient, D is the drag, L is the lift, v_∞ is the air free-stream velocity, c is the chord length of the airfoil, and ρ_∞ is the density of air [9].

The governing equations are written as [10]

$$\frac{\partial \rho}{\partial t} + \frac{\partial}{\partial x_i}(\rho u_i) = 0 \quad Eq.\ 3$$

Reynolds - Averaged Navier-Stokes (RANS) equations is given by:

$$\frac{\partial}{\partial t}(\rho u_i) + \frac{\partial}{\partial x_j}(\rho u_i u_j)$$

$$\frac{\partial p}{\partial x_i} + \frac{\partial}{\partial x_i}\left[\frac{\partial u_i}{\partial x_j} + \frac{\partial u_i}{\partial x_i} - \frac{2}{3}\delta_{ij}\frac{\partial u_l}{\partial x_l}\right]$$
$$+ \frac{\partial}{\partial x_i}(-\rho \overline{u_i u_j}) \quad Eq.\ 4$$

Where the term $-\rho \overline{u_i u_j}$ is the Reynolds stress term. The transport equations of k and ε used in k-ε turbulence model are written as:

$$\frac{\partial}{\partial t}(\rho k) + \frac{\partial}{\partial x_i}(\rho k u_j) = \frac{\partial}{\partial x_i}\left(\alpha_k \mu_{eff}\frac{\partial k}{\partial x_i}\right) + G_k + G_b - \rho s - Y_M + S_k \quad Eq.\ 5$$

$$\frac{\partial}{\partial t}(\rho s) + \frac{\partial}{\partial x_i}(\rho s u_i)$$

$$= \frac{\partial}{\partial x_j}\left[(\mu + \frac{\mu_t}{\sigma_s})\frac{\partial s}{\partial x_j}\right] + \frac{s}{k}(G_k + C_{3s}G_b) - C_{2s}\rho\frac{s^2}{k} + S_s \quad Eq.\ 6$$

The above equations contain 5 adjustable constants $G_{ls} C_{2s} C_\mu \sigma_k$ and σ_s that are the tur- bulent Prandtl numbers for k and ε, respectively, which have default values,
$G_{ls} = 1.44$, $C_{2s} = 1.92$, $C_\mu = 0.09$, $\sigma_k = 1.00$ and $\sigma_s = 1.30$

III. RESULTS AND DISCUSSIONS

Fig. 3(a) shows the pressure distribution over the wind turbine blade at the stall angle of attack. It is obvious that the maximum pressure is generated at the leading edge. The pressure contour clearly shows the creation of negative pressure at the top and bottom surfaces of the wind turbine blade. The lift force results from these two imbalanced forces of negative pressure at both of the surfaces. Increasing the angle of attack up to a certain limit leads to increasing the negative pressure at the top surface whereas de- creasing the negative pressure at the bottom surface, and that is the reason why the lift increases. But after a certain angle of attack, the opposite phenomenon occurs owing to the separation of flow from the upper surface of the airfoil and formation of wake near the trailing edge which ultimately decreases the lift and increases the drag.

Fig. 3(b) shows that the streamlines over the wind turbine blade has started to detach from the upper surface on passing the air over the trailing edge of the wind turbine blade where small vortices are created and consequently creating a small amount of negative pressure. Consequently, the wakes resulting from these vortices and negative pressure near the separation point of the streamlines over the wind turbine blade leads to increasing the drag. Flow separation begins to occur at small angles of attack at the same of dominating the attached flow over the wind turbine blade. As the angle of attack increases, the separated regions on the top of the wind turbine blade increase in size and hinder the wing's ability to create lift. At the critical angle of attack, separated flow is so dominant that further increases in angle of attack produce less lift and vastly more drag.
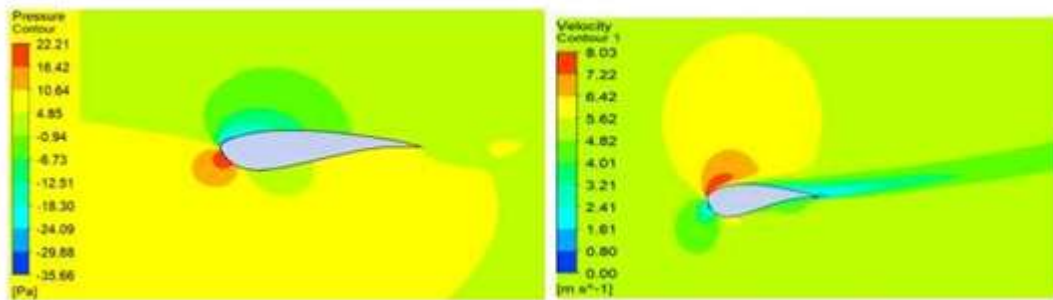

Fig. 3(a). Pressure contour **Fig. 3(b).** Velocity contour

Fig.3 (a) & 3 (b), Pressure & velocity contours of wind turbine blade for stall angle of attack (i.e., 22°) at 5 m/s
The Coefficient of pressure decreases from -0.493 at -4° angle of attack, reaches a low of -0.498 at 0° angle of attack, and then increases with increase in angle of attack to a maximum value of -0.3247 at 30° angle of attack as shown in Figure 4.
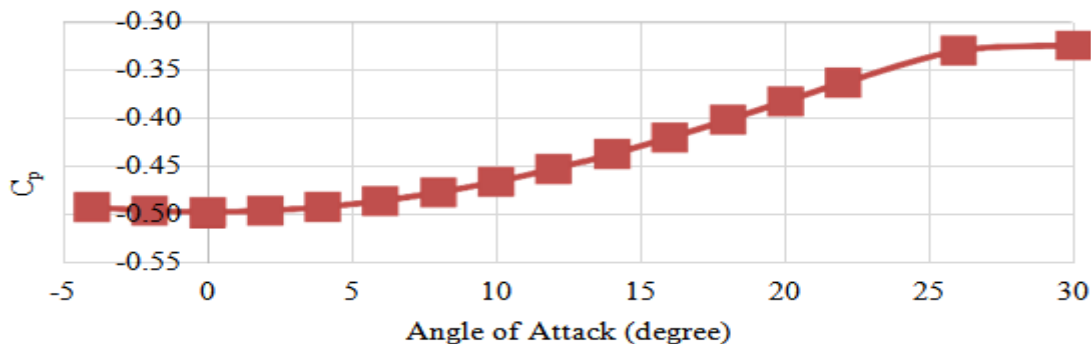
Fig. 4. Coefficient of pressure vs. angle of attack

Figures 5 shows the profiles of the coefficient of lift vs. angle of attack. The lift coefficient increases linearly by increasing the angle of attack (-4° to 30°) and it reaches the maximum at 22° angle of attack. Further increasing the angle of attack, it will lead to stall. The recorded maximum coefficient of lift for wind turbine blade is 0.8447 at 22° stall angle of attack, also termed as the critical angle of attack.
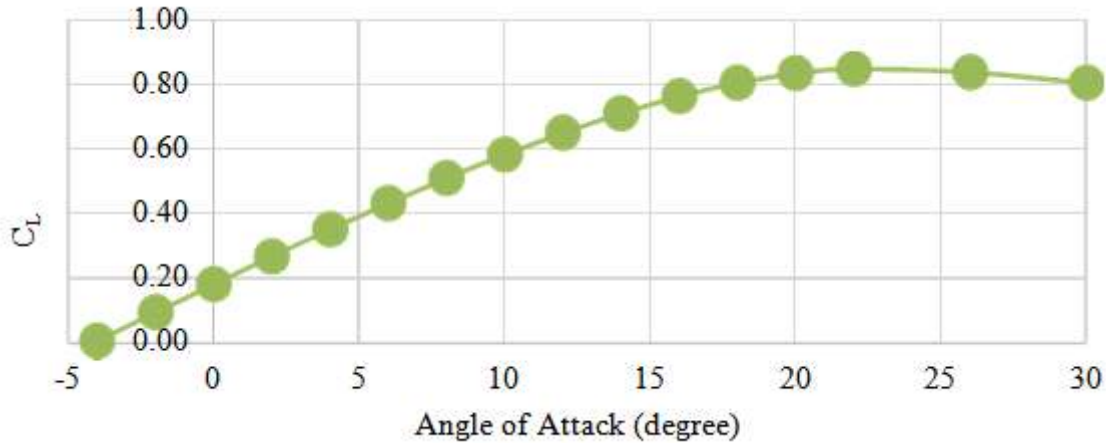
Fig. 5. Coefficient of lift vs. angle of attack

Figure 6 shows the lift/drag ratio (sliding ratio) vs. angle of attack. From the Figure 6, it's evident that the sliding ratio reaches maximum at 8° angle of attack at 5 m/s. After reaching its maximum value, the sliding ratio gradually decreases as the angle of attack increases. It is concluded that, in order to maximise the wind turbine's power output, the operating angle of attack should be between 6° and 10° for wind turbine blade.
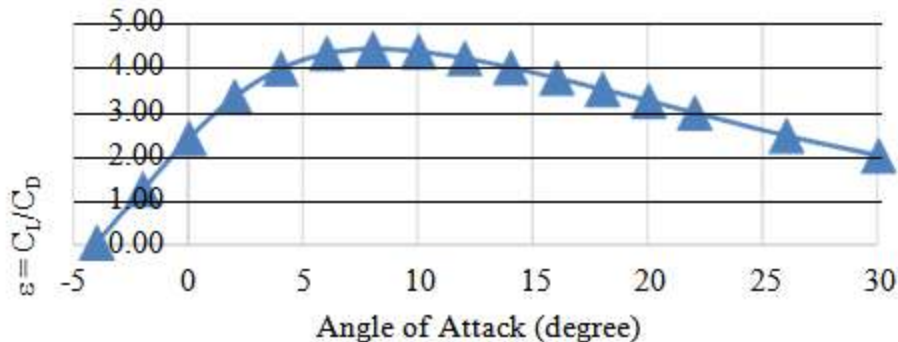
Fig. 6. Sliding ratio vs angle of attack

IV. VALIDATION

The aerodynamic characteristics of wind turbine blade have been numerically inves-tigated at various angle of attack, and aerodynamic performances have been validated with literature (Wind tunnel experimental results) [7]. Figure 7 shows the coefficient of lift versus angle of attack for the wind turbine blade and it is observed that validation process could ultimately result in the discrepancy between the numerical and experi-mental data because the experimental data captured for 2D and numerical simulations carried out for 3D at $Re = 0.68 \times 10^5$. From the literature results, the critical angle of attack is occurred at 14° angle of attack for 2D case. Whereas, for 3D case, the critical angle of attack is occurred at higher angle of attack i.e. 22° angle of attack. The maxi- mum variation of the coefficient of lift from numerical

and literature results at 5 m/s and 14° stall angle of attack is 46.87%.
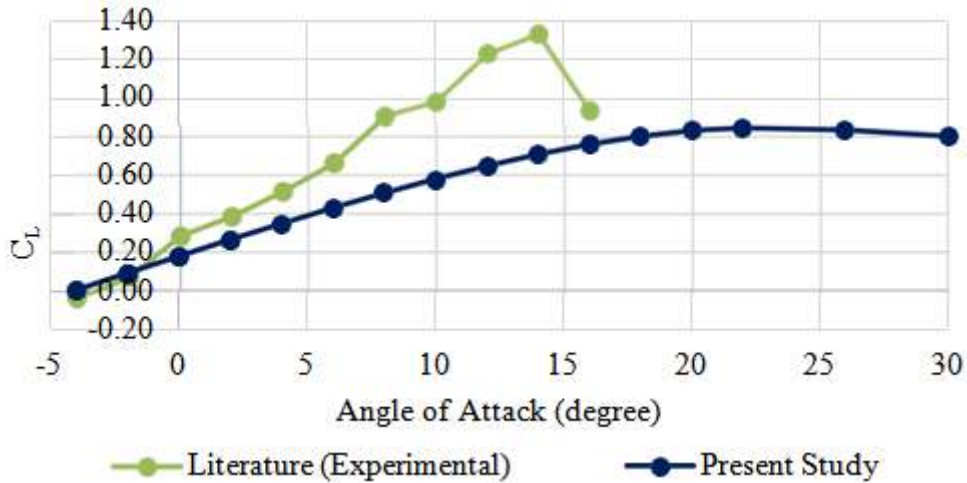

Fig. 7. Coefficient of lift vs angle of attack at 5 m/s

Figure 8 shows the lift/drag ratio (sliding ratio) versus angle of attack for wind turbine blade. The maximum variation of lift/drag ratio (sliding) obtained from numerical and literature at 5 m/s and 8° AOA is 39.98%.
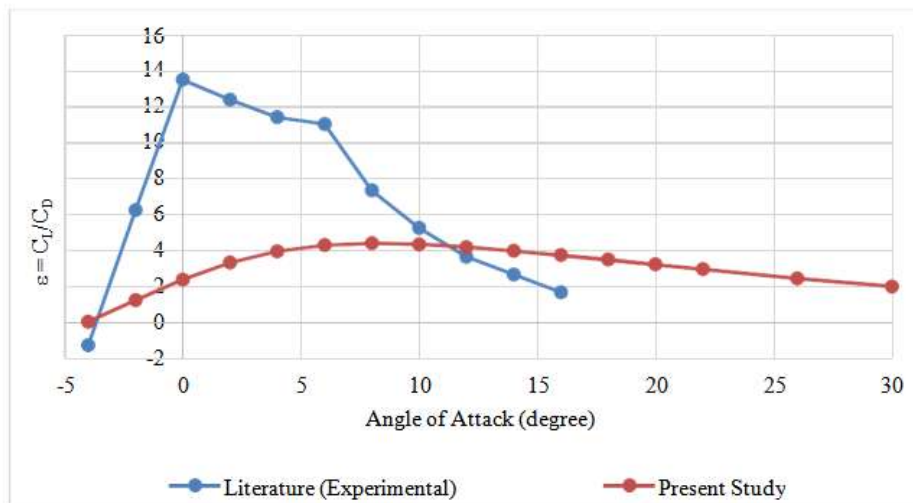

Fig. 8. Computational sliding ratio versus angle of attack curve of wind turbine bladeat 5 m/s.

V. CONCLUSIONS

According to the findings, the sliding ratio is an important factor in determining the effectiveness and usability of a wind turbine blade profile. The optimum angle of attack should lie between 5° to 10° angle of attack to get the maximum sliding ratio and maximum power extracted from the wind turbine blade. It should also be noted that asthe angle of attack exceeds the optimum range, the sliding ratio decreases and the difference in sliding ratios becomes very small. Moreover, it is concluded from the results that the NREL wind turbine profile S821 is the most efficient blade profiles and they are suitable for wind turbines working at low wind speeds.

REFERENCES

[1]. Rohan Kapdi, Rahul Dahiya, Vishal Gangadhar Naranje, 2016, "Analysis and optimi- zation of horizontal axis wind turbine blade profiles", IJRET: International Journal of Research in Engineering and Technology eISSN: 2319-1163 | pISSN: 2321-7308.

[2]. Hansen MO. Aerodynamics of wind turbine. Earthscan, UK and USA; 2008, ISBN: 978-1-84407-438-9.

[3]. Vermeer LJ, Sorensen JN, Crespo A. Wind turbine wake aerodynamics. Progress Aerospace Science 2003; 39:467–510.

[4]. Mohamed A. Sayed, Hamdy A. Kandil, Ahmed Shaltot, 2012, "Aerodynamic analysis of different wind-turbine-blade profiles using finite-volume method", Energy Conver- sion and Management 64 (2012) 541–550. http://dx.doi.org/10.1016/j.enconman.2012.05.030

[5]. Hoogedoorn, E., Jacobs, G.B., Bey, A., 2010. "Aero-elastic behavior of a flexible blade for wind turbine application: a 2D computational study", Elsevier Ltd. J Energy; 35(2):778–85.

[6]. Han Cao, 2011, "Aerodynamics Analysis of Small Horizontal Axis Wind Turbine Blades by Using 2D and 3D CFD Modelling", Thesis submitted to the University of the Central Lancashire.

[7]. M. M. M. Talukder, M. K. Islam, M. R. Rukan, 2016, "Comparative Aerodynamic Analysis of Wind Turbine Blade Profiles", International Journal of Engineering Research & Technology (IJERT) ISSN: 2278-0181 IJERTV5IS010031 www.ijert.org, Vol. 5 Issue 01, January-2016

[8]. https://wind.nrel.gov/airfoils/Documents/S819,S820,S821_Design Date of access: 23/05/2015

[9]. Anderson, J. D., 2011. "Fundamentals of Aerodynamics", Fifth Edition, McGraw-HillCompanies, Inc.

[10]. Somashekar V, & Immanuel Selwyn Raj A, (2021). Comparative Study on the Predic- tion of Aerodynamic Characteristics of Mini - Unmanned Aerial Vehicle with Turbu- lence Models. International Journal of Aviation, Aeronautics, and Aerospace,

[11]. 8(1). https://doi.org/10.15394/ijaaa.2021.1559